DMD Fast Forward. Published on February 24, 2006 as doi:10.1124/dmd.105.007849
This article has not been copyedited and formatted. The final version may differ from this version.

DMD#7849

Oxidative metabolism of the alkaloid rutaecarpine by human cytochrome P450

Yune-Fang Ueng, Ming-Jaw Don, Woan-Ching Jan, Shu-Yun Wang, Li-Kang Ho, and Chieh-Fu Chen

National Research Institute of Chinese Medicine (Y.F.U., M.J.D., S.Y.W., C.F.C.) Department of Pharmacology, National Yang-Ming University (Y.F.U., W.C.J., L.K.H., C.F.C.), Graduate Institute of Medical Sciences, Taipei Medical University (Y.F.U.), Mackey Medicine, Nursing and Management College (W.C.J.), Taipei, Taiwan, R.O.C., and Qing-Dao University, Qing-Dao, China (C.F.C.)

Running title: P450-catalyzed metabolism of rutaecarpine

Send correspondence to:

*Dr. Yune-Fang Ueng

National Research Institute of

Chinese Medicine

155-1, Li-Nong Street, Sec. 2

Taipei 112, Taiwan, R.O.C.

Tel: 886-2-2820-1999 Ext. 6351

Fax: 886-2-2826-4266

E-mail: ueng@nricm.edu.tw

Contents:

Number of text pages: 21

Number of tables: 2

Number of figures: 7

Number of references: 30

Words of abstract: 217

Words of introduction: 455

Words of discussion: 1159

Abbreviations: CYP, P450, cytochrome P450; α-NF, α-naphthoflavone

DMD Fast Forward. Published on February 24, 2006 as DOI: 10.1124/dmd.105.007849
This article has not been copyedited and formatted. The final version may differ from this version.

Abstract

Rutaecarpine is the main active alkaloid of the herbal medicine, *Evodia rutaecarpa*. To identify the major human cytochrome P450 (P450, CYP) participating in rutaecarpine oxidative metabolism, human liver microsomes and bacteria-expressed recombinant human P450 were studied. In liver microsomes, rutaecarpine was oxidized to 10-, 11-, 12-, and 3-hydroxyrutaecarpine. Microsomal 10- and 3-hydroxylation activities were strongly inhibited by ketoconazole. The 11- and 12-hydroxylation activities were inhibited by α-naphthoflavone, quinidine, and ketoconazole. These results indicated that multiple hepatic CYPs including CYP1A2, CYP2D6, and CYP3A4 participate in rutaecarpine hydroxylations. Among recombinant CYPs, CYP1A1 had the highest rutaecarpine hydroxylation activity. Decreased metabolite formation at high substrate concentration indicated that there was substrate inhibition of CYP1A1- and CYP1A2-catalyzed hydroxylations. CYP1A1-catalyzed rutaecarpine hydroxylations had V_{max} values of 1388 ~ 1893 pmol/min/nmol P450, K_m values of 4.1 ~ 9.5 μM, and K_i values of 45 ~ 103 μM. These results indicated that more than one molecule of rutaecarpine is accessible to the CYP1A active site. The major metabolite 10-hydroxyrutaecarpine decreased CYP1A1, CYP1A2 and CYP1B1 activities with respective IC_{50} values of 2.56 ± 0.04, 2.57 ± 0.11, and 0.09 ± 0.01 μM, suggesting that product inhibition might occur during rutaecarpine hydroxylation. The metabolite profile and kinetic properties of rutaecarpine hydroxylation by human CYPs provides important information relevant to the clinical application of rutaecarpine and *E. rutaecarpa*.

Introduction

Rutaecarpine is a main quinazolinocarboline alkaloid isolated from *Evodia rutaecarpa* (Wu-chu-yu), which has been used as a herbal medicine for the treatment of gastrointestinal disorder and headache (Liao et al., 1981; Tang and Eisenbrand, 1992). The remedy containing *E. rutaecarpa* is generally taken orally. The estimated dosage of rutaecarpine from ingestion of Wu-chu-yu tang, a remedy containing *E. rutaecarpa* is about 19 mg/day (Ueng et al., 2002a). Rutaecarpine has a variety of pharmacological actions including antithrombotic, antianoxic, hypotensive, and vasorelaxant effects (Sheu, 1999). Microsomal cytochrome P450 (P450, CYP)-dependent monooxygenase plays a major role in the oxidative metabolism of xenobiotics including drugs and natural products (Guengerich, 1995; Hasler et al., 1999). Our previous reports demonstrated that rutaecarpine was a CYP1A2-selective inhibitor in human liver microsomes (Ueng et al., 2002b). Rutaecarpine was metabolized by rat liver microsomal enzymes to form 10-, 11-, 12-, and 3-hydroxyrutaecarpine (Ueng et al., 2005). Lee et al. (2004) reported that the formation rate of total rat rutaecarpine metabolites was stimulated by P450 inducers, 3-methylcholanthrene and phenobarbital but not by acetone and dexamethasone. 3-Methylcholanthrene, phenobarbital, acetone, and dexamethasone are inducers of CYP1A, CYP2B, CYP2E1, and CYP3A in rats, respectively (Waxman, 1999; Waxman and Azaroff, 1992). These results suggested that CYP1A and CYP2B played main roles in rat rutaecarpine metabolism. However, the main human P450 forms catalyzing rutaecarpine hydroxylations were not identified and the quantification and kinetic analyses were not reported.

In human liver, CYP1A2, CYP2C9, CYP2D6, CYP2E1, and CYP3A4 are the main P450 forms responsible for drug oxidation (Guengerich, 1995). CYP1A2, CYP2C, CYP2D6, CYP2E1, and CYP3A constitute about 13%, 18%, 2%, 7%, and 29% of the total P450 content, respectively (Shimada et al., 1994). CYP2C9 represents about half to 75% of total

DMD Fast Forward. Published on February 24, 2006 as DOI: 10.1124/dmd.105.007849
This article has not been copyedited and formatted. The final version may differ from this version.

CYP2C (Lasker et al., 1998). CYP3A4 is the most abundant P450 form in human liver samples. CYP1A1 and CYP1B1 are expressed in low levels in human liver, but are inducible in the liver and play important roles in the activation of pro-toxins in induced liver and extrahepatic tissues. CYP2B6 constitutes about 0.2% of the total hepatic P450 content. Although the content of CYP2B6 was low in human liver, CYP2B6 was studied due to its main role in rat rutaecarpine hydroxylation (Lee et al., 2004). α-Naphthoflavone (α-NF), orphenadrine, sulfaphenazole, quinidine, 4-methylpyrazole, and ketoconazole preferentially inhibited CYP1A2, CYP2B6, CYP2C9, CYP2D6, CYP2E1, and CYP3A4 activities, respectively (Balawin et al., 1995; Bourrie et al., 1996; Chang et al., 1994). Thus, to identify the P450 forms participating in human rutaecarpine hydroxylations, the effects of P450 inhibitors were analyzed using human liver microsomes, and rutaecarpine hydroxylation activities were determined using *Escherichia coli* membranes expressing human P450s. Among expressed P450 forms, our results showed that CYP1A1 had the highest activity. The kinetic parameters of CYP1-catalyzed hydroxylations were determined.

Methods

Chemicals

Rutaecarpine was synthesized following the method of Bergman and Bergman (1985). Glucose-6-phosphate (G6P), G6P dehydrogenase, ketoconazole, 4-methylpyrazole, NADP, α-NF, orphenadrine, quinidine, and sulfaphenazole were purchased from Sigma-Aldrich Inc. (St. Louis, MO, U.S.A.). The standards for metabolites, 10-, 11-, 12-, and 3-hydroxyrutaecarpine were synthesized from corresponding methoxyrutaecarpines as described in previous report (Ueng et al., 2005).

Microsomal preparation and bicistronic human P450 Expression

Four Chinese Liver samples (HL1-4) were obtained from patients who underwent liver resection in National Taiwan University Hospital (Taipei, Taiwan). Four Caucasian liver samples (HL5-8) were obtained from Dr. F. Peter Guengerich through Tennessee Donor Services (Nashville, TN, U.S.A.). Microsomes of frozen human liver samples were prepared following the method of Guengerich (1994). Bicistronic human P450 plasmids were kindly provided by Dr. F. Peter Guengerich (Vanderbilt University, Nashville, TN, U.S.A.). P450 constructs consisting of the coding sequence of a P450 followed by that of NADPH-P450 reductase were transformed to *E. coli* DH5α by electroporation. Bacterial membrane fractions were prepared following the method of Parikh et al. (1997). Microsomes and bacterial membrane fractions were stored at -75°C until use.

Enzyme assays

Microsomal protein concentration was determined by the method of Lowry et al. (1951). P450 content was measured by the spectrophotometric method of Omura and Sato (1964). 7-Ethoxyresorufin *O*-deethylation activity was determined by measuring the fluorescence of resorufin (Pohl and Fouts, 1980). Rutaecarpine hydroxylation activity was determined as described before (Ueng et al., 2005). Incubation mixtures (1 ml total vol.) contained 1 mg/ml microsomal protein, a NADPH-generating system, and various concentrations of rutaecarpine as indicated in the Results. The NADPH-generating system consisted of 10 mM G6P, 0.5 mM NADP, and 0.25 u/ml G6P dehydrogenase. For *E. coli* membranes expressing human CYP1, 20 pmol P450 was added in the assay. For membranes expressing human CYP2A6, CYP2C9, CYP2D6, CYP2E1, and CYP3A4, 100 pmol P450 was added in the assay. Hydroxylation metabolites were separated by HPLC using a C18 column (4.6 X 250 mm, 5 μm, Agilent, U.S.A. or 5C18-MS-II, Cosmosil, U.S.A.) and a mobile phase containing 10% methanol and 26% acetonitrile in 0.04% formic acid at a flow

rate of 1 ml/min. An UV detector L-7420 (Hitachi Ltd., Tokyo, Japan) was used and metabolites were detected by measuring the absorbance at 344 nm. The amounts of hydroxyrutaecarpines were determined using synthetic standards. Orphenadrine and 4-methylpyrazole were dissolved in water. α-NF, sulfaphenazole, quinidine, and ketoconazole were dissolved in ethanol. For the inhibition study, the concentrations of α-NF, orphenadrine, sulfaphenazole, quinidine, 4-methylpyrazole, and ketoconazole were 10, 300, 1, 10, 20, and 1 μM in the assay, respectively. The final concentration of ethanol was less than 0.4%. The same concentration of ethanol was added in the control incubation.

Binding spectral analysis

Binding spectra were analyzed by using tandem cuvettes, which have two separate chambers in one cuvette. Various concentrations of 10-hydroxyrutaecarpine and *E. coli* membrane suspension containing 0.2 μM P450 in 0.1 M potassium phosphate buffer, pH7.4 were added in both sample and reference cuvettes at room temperature. In the reference cuvette, *E. coli* membrane suspension and 10-hydroxyrutaecarpine in potassium phosphate buffer were kept separated in two chambers. After mixing *E. coli* membrane suspension with 10-hydroxyrutaecarpine in the sample cuvette, the difference spectrum was recorded from 350 nm to 450 nm. The spectral dissociation constant (K_s) and maximal absorbance change ($\triangle A_{max}$) were calculated by non-linear regression without weight according to the equation $\triangle A = I \cdot \triangle A_{max} / (K_s + I)$, where I is the inhibitor concentration (Sigma Plot, Jandel Scientific, San Rafael, CA, USA).

Data and statistical analyses

Substrate inhibition can be regarded as a form of uncompetitive inhibition (Houston and Kenworthy, 2000). Thus, kinetic parameters of CYP1A1-catalyzed rutaecarpine

DMD Fast Forward. Published on February 24, 2006 as DOI: 10.1124/dmd.105.007849
This article has not been copyedited and formatted. The final version may differ from this version.

hydroxylations were calculated according to uncompetitive inhibition by substrate. Values of velocities (v) at various substrate concentrations (S) were fit using nonlinear least-squares regression without weight due to the equation: $v = V_{max}*S/(K_m+S(1+S/K_i))$, where V_{max} and K_i are the maximal velocity and inhibition constant, respectively (Sigma Plot, Jandel Scientific, San Rafael, CA, U.S.A.). The concentrations of chemicals required for 50% inhibition of 7-ethoxyresorufin *O*-deethylation activity (IC_{50}) were calculated by curve fitting (Grafit, Erithacus Software Ltd., Staines, UK). For inhibitory kinetic analysis, values of velocities (v) at various substrate concentrations (S) were fit using nonlinear least-squares regression without weight due to the equation, consistent with the competitive inhibition according to the Michaelis-Menten equation: $v = V_{max}*S/(K_m[1 + (I/K_i)] + S)$, where I and K_i are the inhibitor concentration and inhibition constant, respectively (Sigma Plot, Jandel Scientific, San Rafael, CA, USA). The significant relationship of pairs of variables was analyzed by Spearman rank correlation test using the software Sigma Stat 2.03 (SPSS, Inc., Chicago, IL, U.S.A.). A p value < 0.05 was considered statistically significant.

Results

Rutaecarpine hydroxylation by human liver microsomes

Rutaecarpine was oxidized by human liver microsomal enzymes to form mainly 10-, 11-, 12-, and 3-hydroxyrutaecarpine (Fig. 1). In eight human liver samples, rutaecarpine 10-, 11-, 12-, and 3-hydroxylation activities were in the range (mean ± SE) of 7.1 ~ 43.9 (25.9 ± 4.7), 8.5 ~ 32.8 (22.3 ± 3.0), not detectable ~ 13.3 (5.4 ± 1.6), and 5.0 ~ 23.0 (14.1 ± 2.5) pmol/min/mg protein, respectively. Except for the high 11-hydroxylation activity of HL8 sample, 10-hydroxyrutaecarpine was the most abundant product in human liver samples. Individual differences were as high as 6-, 4-, and 5-fold in 10-, 11-, and

3-hydroxyrutaecarpine formation, respectively. The formation of 12-hydroxyrutaecarpine by HL2 and HL3 microsomes were under the detection limit. α-NF caused 54%, 60%, and 51% decreases of 11-, 12-, and 3-hydroxylation activities, respectively (Table 1). In contrast, the inhibition of 10-hydroxylation by α-NF was less than 30%. Quinidine decreased 10-, 11-, 12-, and 3-hydroxylation activities by 55%, 53%, 55%, and 58%, respectively. Ketoconazole decreased 10-hydroxyrutaecarpine formation by 86% and 3-hydroxyrutaecarpine by 78%. However, orphenadrine, sulfaphenazole, and 4-methylpyrazole caused less than 30% decreases.

Rutaecarpine hydroxylation by human P450 forms

At rutaecarpine concentration less than 50 μM in the assay, some P450-catalyzed rutaecarpine hydroxylations were under the detection limit. Thus, 50 μM rutaecarpine was used in the assay of all bicistronic human P450 forms determined. Hydroxylation product formation was linear at CYP1A1 and CYP1A2 concentrations in the range of 1 to 20 pmol P450/ml (Fig. 2). However, at the concentrations higher than 20 pmol P450/ml, the activities approached the plateau due to substrate saturation. For CYP2C9, CYP2D6, and CYP3A4, hydroxylation was linear at P450 concentrations up to 100 pmol P450/ml. Thus, 20 pmol P450/ml was used in the assay of CYP1 members and 100 pmol P450/ml was used in the assay of the other CYPs. Rutaecarpine hydroxylation by CYP1A1 was linear with the incubation time up to 20 min (Fig. 3). Thus, the formation of hydroxylation products was determined at 20 min incubation. HPLC analysis of rutaecarpine hydroxylation products showed that CYP1A1-catalyzed hydroxylation formed 10-, 11-, 12-, and 3-hydroxyrutaecarpine (Fig. 1). Determination of rutaecarpine hydroxylation by *E. coli* membrane expressing human P450 showed that CYP1A1 had the highest 10-, 11-, 12-, and 3-hydroxylation activities (Table 2). 10-Hydroxyrutaecarpine was the most abundant

DMD Fast Forward. Published on February 24, 2006 as DOI: 10.1124/dmd.105.007849
This article has not been copyedited and formatted. The final version may differ from this version.

metabolite of rutaecarpine hydroxylation by CYP1A1. CYP1A2 had rutaecarpine 11-, 12-, and 3-hydroxylation activity. In contrast, no 10-hydroxyrutaecarpine was detected. CYP1B1 had rutaecarpine 10- and 3-hydroxylation activities. However, an additional peak appeared at 14 min, which also appeared as a metabolite by some human liver samples (Fig. 1A (B)). The structure of this metabolite was not identified. Rutaecarpine 10-, 11-, 12-, and 3-hydroxylation activities were detected with CYP2C9 and CYP2D6. CYP2E1 showed rutaecarpine 11-hydroxylation activity and CYP3A4 showed rutaecarpine 10- and 3-hydroxylation activities. In contrast, CYP2A6 had no detectable rutaecarpine hydroxylation activity.

Kinetic analysis of CYP1-catalyzed rutaecarpine hydroxylation

For CYP1A1-catalyzed rutaecarpine hydroxylation, the velocities decreased at rutaecarpine concentration higher than 25 μM (Fig. 4A). At low concentration of rutaecarpine ($\leq$ 5 μM), the plot did not follow a hyperbolic pattern (Fig. 4B). The Lineweaver-Burk plot of CYP1A1-catalyzed rutaecarpine hydroxylation showed a non-linear pattern (Fig. 4C). Kinetic analysis was performed according to the substrate inhibition pattern as described in Methods. The results generated kinetic parameters of CYP1A1 for each hydroxylation as follows: 10-hydroxylation: V_{max} = 1799 ± 326 pmol/min/nmol P450, K_m = 5.1 ± 2.0 μM, K_i = 103 ± 53 μM (r = 0.97); 11-hydroxylation: V_{max} = 1535 ± 292 pmol/min/nmol P450, K_m = 4.1 ± 1.8 μM, K_i = 105 ± 61 μM (r = 0.96); 12-hydroxylation: V_{max} = 1388 ± 350 pmol/min/nmol P450, K_m = 4.6 ± 2.6 μM, K_i = 91 ± 60 μM (r = 0.95); 3-hydroxyrutaecarpine: V_{max} = 1893 ± 607 pmol/min/nmol P450, K_m = 9.5 ± 5.1 μM, K_i = 45 ± 27 μM (r = 0.97). The Eadie-Hofstee plot showed a convex curve indicating positive cooperation (Fig. 4D). At a substrate concentration higher than 10 μM, the Hill's plot did not show linearity (Fig. 4E). At the linear range (0.75 - 8 μM), results of linear regression showed cooperativities of 1.6 (r = 0.96), 1.7 (r = 0.96), 1.4

(r = 0.96), and 1.5 (r = 0.99) for 10-, 11-, 12-, and 3-hydroxylation, respectively (Fig. 4E, insert plot).

Determination of the relationship between rutaecarpine concentrations and CYP1A2-catalyzed hydroxylation activities showed that activity decreased at a rutaecarpine concentration higher than 100 μM (Fig. 5A). The hydroxylation activity of CYP1A2 also showed substrate inhibition at a high rutaecarpine concentration. In contrast to CYP1A1 and CYP1A2, there was no substrate inhibition observed in CYP1B1-catalyzed rutaecarpine 10-hydroxylation (Fig. 5B).

Inhibition of CYP1 enzymes by the metabolite 10-hydroxyrutaecarpine

10-Hydroxyrutaecarpine inhibited CYP1A1-, CYP1A2-, and CYP1B1-catalyzed 7-ethoxyresorufin *O*-deethylation activity with IC_{50} values of 2.56 ± 0.04, 2.57 ± 0.11, and 0.09 ± 0.01 μM, respectively. Among CYP1 enzymes, 10-hydroxyrutaecarpine had the highest inhibitory effect on CYP1B1. 10-Hydroxyrutaecarpine was a competitive inhibitor of CYP1B1 with a K_i value of 0.11 ± 0.02 μM (r = 0.99, Fig. 6A and B). The binding of 10-hydroxyrutaecarpine to CYP1B1 exhibited a binding spectra with an absorbance maxima at 377 nm and a minimum at 417 nm (Fig. 6C). The absorbance change (377-417 nm) was unsaturable and showed a linear relationship with 10-hydroxyrutaecarpine concentration in a range of 0.01 – 9.0 μM (r = 0.97) (Fig. 6C and D).

Discussion

Our previous report demonstrated that the alkaloid rutaecarpine was oxidized by rat liver microsomes to form 10-, 11-, 12-, and 3-hydroxyrutaecarpine (Ueng et al., 2005). In this report, our results revealed that rutaecarpine was also oxidized by human liver microsomal

enzymes to form 10-, 11-, 12-, and 3-hydroxyrutaecarpine (Fig. 1). This is the first report to determine human metabolism of rutaecarpine *in vitro*. The results of microsomal inhibition were consistent with hydroxylation activities of bacterial membranes expressing bicistronic human P450s. Microsomal 10-hydroxylation activity was strongly inhibited by quinidine and ketoconazole (Table 1). Consistent with this inhibition result, *E.coli*-expressed human CYP2D6 and CYP3A4 had 10-hydroxylation activities higher than those of the other P450 enzymes (Table 2). Microsomal 12-hydroxylation was inhibited by α-NF, quinidine, and ketoconazole. Human CYP1A2, CYP2C9, and CYP2D6 had detectable 12-hydroxylation activities (Table 2). Microsomal 11-hydroxylation was inhibited by α-NF, quinidine, and ketoconazole. Human CYP1A2 and CYP2D6 had higher 11-hydroxylation activities than the other CYPs. However, CYP3A4 had no detectable 11-hydroxylation activity. Microsomal 3-hydroxylation was inhibited by α-NF, quinidine, and ketoconazole. 3-Hydroxylation activities of CYP2D6 and CYP3A4 were higher than those of the other CYPs. However, CYP1A2 had relatively low 3-hydroxylation activity.

Thus, to further clarify the roles of CYP1A2 and CYP3A4 in rutaecarpine hydroxylations, correlation analysis (Spearman rank order correlation) was carried out to delineate the association of rutaecarpine hydroxylation with CYP1A2- and CYP3A4-catalyzed model reactions. Correlation analysis showed that liver microsomal rutaecarpine 11- and 12-hydroxylation activities had significant correlation ($p < 0.05$) with CYP1A2 model reaction, 7-methoxyresorufin *O*-demethylation activity (correlation coefficient (r) values of 0.857 and 0.762, respectively). In contrast, rutaecarpine 10- and 3-hydroxylation activities were not significantly correlated with 7-methoxyresorufin *O*-demethylation activity ($r = 0.190$ and 0.357, respectively). Liver microsomal rutaecarpine 10- and 3-hydroxylation activities were significantly correlated with the CYP3A4 model reaction, nifedipine oxidation activity (r values of 0.943 and 0.886, respectively). In contrast,

DMD Fast Forward. Published on February 24, 2006 as DOI: 10.1124/dmd.105.007849
This article has not been copyedited and formatted. The final version may differ from this version.

rutaecarpine 11- and 12-hydroxylation activities had no significant correlation with nifedipine oxidation activity (r = -0.029 and 0.429, respectively). These results were consistent with the rutaecarpine hydroxylation activities of recombinant human P450. In contrast, orphenadrine, sulfaphenazole, and 4-methylpyrazole decreased microsomal 10-, 11-, 12-, and 3-hydroxylation by less than 30%, suggesting that CYP2B6, CYP2C, and CYP2E1 do not play main roles in human rutaecarpine hydroxylations (Table 1). Although CYP2C9 had detectable rutaecarpine 10-, 11-, 12-, and 3-hydroxylation activities (Table 2), the activities of CYP2C9 may not be high enough for sulfaphenazole to cause inhibition in human liver microsomes. Similar to CYP2C9, CYP2E1 also had low 11-hydroxylation activity. Thus, the P450 enzymes, whose selective inhibition decreased hydroxylation by more than 50% and showed high hydroxylation activities, were identified as the main P450 forms involved in each hydroxylation reaction in human liver (Fig. 7). For rutaecarpine metabolism, CYP2D6 and CYP3A4 were involved in the 10-hydroxylation, CYP1A2 and CYP2D6 in 11-hydroxylation, CYP2D6 in 12-hydroxylation, and CYP2D6 and CYP3A4 in 3-hydroxylation. These results revealed the regio-selective hydroxylation by P450 enzymes.

Among CYPs, our results showed that CYP1A1 had the highest rutaecarpine 10-, 11-, 12-, and 3-hydroxylation activities (Table 2). Our previous report demonstrated that rutaecarpine inhibited CYP1A1- and CYP1A2-catalyzed 7-ethoxyresorufin *O*-deethylation activities (Don et al., 2003). The IC_{50} value of rutaecarpine for CYP1A2 was only 8% of that for CYP1A1 (Don et al., 2003). This strong CYP1A2 inhibition may result in relatively low rutaecarpine oxidation activity of CYP1A2 (Table 2). Kinetic analysis revealed that substrate inhibition occurred for both CYP1A1- and CYP1A2-catalyzed rutaecarpine hydroxylations (Fig. 4A and 5A). At a rutaecarpine concentration higher than 25 μM, hydroxylation activities decreased. In the *in vitro* systems, the pharmacologically active concentrations of rutaecarpine were in the range of 0.1-200 μM (Chen et al., 2002; Sheu, 1999). Substrate

inhibition is possible at high pharmacologically active concentrations. The hydroxylations by CYP1A1 had K_i values 5- to 26-fold higher than K_m values. Substrate inhibition can be due to a variety of mechanisms including allosteric interaction and multiple active sites (Lin et al., 2001). For most P450-catalyzed oxidations, substrate inhibition was partial, suggesting that the substrate inhibition was due to the binding of a second molecule of substrate to the P450-substrate complex to form a poorly productive or nonproductive enzyme complex and reduce the oxidation rates (Lin et al., 2001). Consistent with this allosteric interaction in substrate inhibition, rutaecarpine strongly inhibited CYP1A2-catalyzed 7-ethoxyresorufin *O*-deethylation activity in a mixed type of noncompetitive and uncompetitive inhibition. The K_i value for CYP1A2-substrate complex was less than that for CYP1A2 only, suggesting a strong binding of rutaecarpine to CYP1A2-substrate complex (unpublished result). Besides ~~of~~ CYP1A1 and CYP1A2, rutaecarpine also inhibited CYP1B1-catalyzed 7-ethoxyresorufin *O*-deethylation noncompetitively with an IC_{50} value about 3-fold higher than that for CYP1A2, suggesting that rutaecarpine bound to CYP1B1 and CYP1B1-substrate complexes with similar dissocation constants (Don et al., 2003). However, CYP1B1 did not show the substrate inhibition as obviously as CYP1A1 and CYP1A2.

10-Hydroxyrutaecarpine was the most abundant metabolite formed by most human liver samples. Among CYP1 members, CYP1A1 and CYP1B1 oxidized rutaecarpine to form mainly 10-hydroxyrutaecarpine. For CYP1A1, the plot of velocity *versus* substrate concentration at the concentration less than 10 μM showed a sigmoidal pattern (Fig. 4B). Eadie-Hofstee and Hill plots showed a kinetic pattern with cooperativity higher than 1 for CYP1A1-catalyzed rutaecarpine 10-, 11-, 12-, and 3-hydroxylations (Fig. 4D and E). The positive cooperativity seen in the sigmoidal velocity *vs* substrate concentration plot could be attributed to several factors. These factors include that more than one substrate binding site or conformation is present in CYP1A1 and/or product inhibition (Duggleby, 1994). Thus, the

DMD Fast Forward. Published on February 24, 2006 as DOI: 10.1124/dmd.105.007849
This article has not been copyedited and formatted. The final version may differ from this version.

effect of 10-hydroxyrutaecarpine on CYP1 members were studied. 10-Hydroxyrutaecarpine strongly inhibited CYP1A1-, CYP1A2-, and CYP1B1-catalyzed 7-ethoxyresorufin *O*-deethylation activities with the IC_{50} values in the order of CYP1A1 ≈ CYP1A2 > CYP1B1. The inhibition of CYP1 by this oxidation product may shift the velocity *versus* substrate concentration plot to a sigmoidal pattern. In the future, it will be of interest to determine the plasma concentrations of 10-hydroxyrutaecarpine and/or its conjugates to assess the role of 10-hydroxyrutaecarpine in drug interactions of the rutaecarpine containing remedy in our previous report (Ueng et al., 2003).

The major finding is that multiple P450 enzymes, including CYP1A2, CYP2D6, and CYP3A4 participated in human liver microsomal rutaecarpine hydroxylation (Fig. 7). Genetic variations of CYP1A2, CYP2D6, and CYP3A4 have been reported in humans (Hasler et al., 1999). To clarify the possible individual differences in pharmacological response to *E. rutaecarpa* due to differential metabolic capacity, it will be of interest to investigate the pharmacological effects of rutaecarpine metabolites. The main pharmacological targets of rutaecarpine are the cardiovascular and circulation systems. The pharmacological effects of rutaecarpine may show tissue-specificity. Among the P450 enzymes studied here, CYP1A1 had 10-, 11-, 12-, and 3-hydroxylation activities 6~26-, 6~9-, 10~16-, and 7~27-fold higher than the activities of the other CYPs, respectively. CYP1A1 is essentially extrahepatic and is inducible in the endothelial cells of blood vessels (Ding and Kaminsky, 2003; Dey et al., 1999). Therefore, CYP1A1 may also play an important role in the toxicity and pharmacological activities of rutaecarpine in extrahepatic tissues.

Acknowledgements

We thank Dr. Ta-Liang Chen and Dr. F. Peter Guengerich for providing human liver samples.

References

Balawin SJ, Bloomer JC, Smith GJ, Ayrton AD, Clarke SE, Chenery RJ (1995) Ketoconazole and sulphaphenazole as the respective selective inhibitors of P4503A and 2C9. *Xenobiotica* 25:261-270.

Bergman J and Bergman S (1985) Studies of rutaecarpine and related quinazolinocarboline alkaloids. *J Org Chem* 50:1246-1255.

Bourrie M, Meunier V, Berger Y, and Fabre G (1996) Cytochrome P450 isoform inhibitors as a tool for the investigation of metabolic reactions catalyzed by human liver microsomes. *J Pharmacol Exp Ther* 277:321-332.

Chang TKH, Gonzalez FJ, and Waxman DJ (1994) Evaluation of triacetyloleandomycin, α-naphthoflavone and diethyldithiocarbamate as selective chemical probes for inhibition of human cytochromes P450. *Arch Biochem Biophys* 311:437-442.

Chen CF, Chiou WF, Chou CJ, Liao JF, Lin LC, Wang GJ, and Ueng YF (2002) Pharmacological effects of *Evodia rutaecarpa* and its bioactive components. *Chin Pharm J* 54:419-435.

Dey A, Jones JE, and Nebert DW (1999) Tissue- and cell type-specific expression of cytochrome P450 1A1 and cytochrome P450 1A2 mRNA in the mouse localized in situ hybridization. *Biochem Pharmacol* 58:525-537.

Ding X and Kaminsky LS (2003) Human extrahepatic cytochrome P450: function in

xenobiotic metabolism and tissue-selective chemical toxicity in the respiratory and gastrointestinal tracts. *Ann Rev Pharmacol Toxicol* 43:149-173.

Don MJ, Lewis DFV, Wang SY, Tsai MW, and Ueng YF (2003) Effect of structural modification on the inhibitory selectivity of rutaecarpine derivatives on human CYP1A1, CYP1A2, and CYP1B1. *Bioorg Med Chem Lett* 13:2535-2538.

Duggleby RG (1994) Product inhibition of reversible enzyme-catalysed reactions. *Biochim Biophys Acta* 1209:238-240.

Guengerich FP (1994) Preparation of microsomal and cytosolic fractions. In: *Principles and Methods of Toxicology,* 3rd ed. (Hayes AW ed) pp 1267-1268, Paven Press, New York.

Guengerich FP (1995) Human cytochrome P450 enzymes. In: *Cytochrome P450* (Ortiz de Montellano PR ed) pp. 473-535, Plenum Press, New York and London.

Hasler JA, Estabrook R, Murray M, Pikuleva I, Watreman M, Capdevila J, Holla V, Helvig C, Falck JR, Farrell G, Kaminsky LS, Spivack SD, Boitier E, and Beaune P (1999) Human cytochrome P450. *Mol Aspect Med* 20:1-137.

Houston JB and Kenworthy KE (2000) In vitro-in vivo scaling of CYP kinetic data not consistent with the classical Michaelis-Menten model. *Drug Metab Dispos* 28:246-254.

Lasker JM, Wester MR, Aramsombatdee E, and Raucy JL (1998) Characterization of CYP2C19 and CYP2C9 from human liver: respective roles in microsomal tolbutamide,

S-mephenytoin, and omeprazole hydroxylations. *Arch Biochem Biophys* 353:16-28.

Lee SK, Kim NH, Lee J, Kim DH, Lee ES, Choi HG, Chang HW, Jahng Y, and Jeong TC (2004) Induction of cytochrome P450s by rutaecarpine and metabolism of rutaecarpine by cytochrome P450s. *Planta Med* 70:753-757.

Liao JF, Chen CF, and Chow SY (1981) Pharmacological studies of Chinese herbs. 9. Pharmacological effects of *Evodiae fructus. J Formosa Med Assoc* 79:30-38.

Lin Y, Lu P, Tang C,Mei Q, Sandig G, Rodrigues AD, Rushmore TH, and Shou M (2001) Substrate inhibition kinetics for cytochrome P450-catalyzed reactions. *Drug Metab Dispos* 29:368-374.

Lowry OH, Roseborough NJ, Farr AL, and Randall RL (1951) Protein measurement with the Folin phenol reagent. *J Biol Chem* 193:265-275.

Omura T and Sato R (1964) The carbon monoxide-binding pigment of liver microsomes. 1. Evidence for its hemeprotein nature. *J Biol Chem* 239:2370-2379.

Parikh A, Gillam EMJ, and Guengerich FP (1997) Drug metabolism by *Escherichia coli* expressing human cytochrome P450. *Nat Biotech* 15:784-788.

Pohl RJ andFouts JR (1980) A rapid method for assaying the metabolism of 7-ethoxyresorufin by microsomal subcellular fractions. *Anal Biochem* 107:150-155.

Sheu JR (1999) Pharmacological effects of rutaecarpine, an alkaloid isolated from *Evodia rutaecarpa*. *Cardiovasc Drug Rev* 17:237-245.

Shimada T, Yamazaki H, Mimura M, Inui Y, and Guengerich FP (1994) Interindividual variations in human liver cytochrome P-450 enzymes involved in the oxidation of drugs, carcinogens and toxic chemicals: studies with liver microsomes of 30 Japanese and 30 Caucasians. *J Pharmacol Exp Ther* 270:414-423.

Tang W and Eisenbrand G (1992) Evodia rutaecarpa (Juss) Benth, In: *Chinese Drugs of Plant Origin* (Tang W and Eisenbrand G eds) pp 509-514, Springer-Verlag, Berlin.

Ueng YF, Don MJ, Peng HC, Wang SY, Wang JJ, and Chen CF (2002a) Effects of *Wu-chu-yu tang* and its component herbs on drug-metabolizing enzymes. *Jpn J Pharmacol* 89:267-273.

Ueng YF, Jan WC, Lin LC, Chen TL, Guengerich FP, and Chen CF (2002b) The alkaloid rutaecarpine is a selective inhibitor of cytochrome P450 1A in mouse and human liver microsomes. *Drug Metab Dispos* 30:349-353.

Ueng YF and Wang SY (2003) The herbal preparation Wu-chu-yu-tang enhances the excretion of the CYP1A2 substrate caffeine in mice. *J Chin Med* 14:175-181.

Ueng YF, Yu HJ, Lee CH, Peng C, Jan WC, Ho LK, Chen CF, and Don MJ (2005) Identification of microsomal oxidation metabolites of rutaecarpine, a main active alkaloid of the medicinal herb *Evodia rutaecarpa*. *J Chrom A* 1076:103-109.

Waxman DJ (1999) P450 gene induction by structurally diverse xenochemicals: central role of nuclear receptor CAR, PXR, and PPAR. *Arch Biochem Biophys* 369:11-23.

Waxman DJ and Azaroff L (1992) Phenobarbital induction of cytochrome P-450 gene expression. *Biochem J* 281:577-592.

Footnotes: This work was supported by NSC 91-2320-B077-010 and National Research Institute of Chinese Medicine, Taiwan.

Legends

Figure 1. A. The HPLC chromatograms of rutaecarpine hydroxylation metabolites by recombinant human CYP1A1 ((A)) and human liver microsomes (B). Metabolites, 10-, 11-, 12-, and 3-hydroxyrutaecarpine appeared at 16, 20, 31, and 35 min, respectively. Microsomes were prepared and activities were determined as described in the Methods. Panel (B) shows the chromatogram of microsomal hydroxylation metabolites by human liver samples HL1. B. Microsomal rutaecarpine hydroxylation activities of human liver samples. Results represent the mean of duplicated determinations.

Figure 2. Relationship between rutaecarpine hydroxylation activity and P450 concentrations in the assay. Rutaecarpine hydroxylation activity of bacterial membrane expressing CYP1A1 (●), CYP1A2(▲), CYP1B1(□),, CYP2C9(■), CYP2D6(•), and CYP3A4 (○) was determined using 50 μM rutaecarpine in the reaction mixture.

Figure 3. Relationship between CYP1A1-catalyzed rutaecarpine hydroxylation and the incubation time of the assay. Rutaecarpine hydroxylation activity of bacterial membrane expressing CYP1A1 was determined using 20 pmol P450 and 50 μM rutaecarpine in the reaction mixture. The formation rates of 10-hydroxyrutaecarpine (●), 11-hydroxyrutaecarpine (■), 12-hydroxyrutaecarpine (◆), and 3-hydroxyrutaecarpine (▲) were determined. Results represent the means of duplicate determinations.

Figure 4. Kinetic analyses of rutaecarpine hydroxylations by human CYP1A1. (A) velocity (v) *versus* of rutaecarpine concentration (S) plot of CYP1A1-catalyzed rutaecarpine hydroxylation. (A) velocity (*v*) *versus* of rutaecarpine concentration (*S*) plot of

CYP1A1-catalyzed rutaecarpine hydroxylation. Lines show the best fit as determined by nonlinear least-squares regression according to substrate inhibition as described in the Methods. (B) velocity (*v*) *versus* of rutaecarpine concentration (*S*) plots of CYP1A1-catalyzed rutaecarpine hydroxylations at rutaecarpine concentration less than 10 μM. (C) Lineweaver-Burk plots of CYP1A1-catalyzed rutaecarpine hydroxylations. Lines show the best fit as determined by nonlinear least-squares regression according to substrate inhibition. (D) The plots of *v versus v*/*S* (Eadie-Hofstee plot). (E) The plots of log(v/V_{max}-v) *versus* log*S* (Hill plot). The formation rates of 10-hydroxyrutaecarpine (●), 11-hydroxyrutaecarpine (■), 12-hydroxyrutaecarpine (◆), and 3-hydroxyrutaecarpine (▲) were determined. Results represent the means of duplicate determinations.

Figure 5. The velocity (*v*) *versus* of rutaecarpine concentration (*S*) plots of CYP1A2- (A) and CYP1B1- (B) catalyzed rutaecarpine hydroxylation. The formation rates of 10-hydroxyrutaecarpine (●), 11-hydroxyrutaecarpine (■), 12-hydroxyrutaecarpine (◆), and 3-hydroxyrutaecarpine (▲) were determined. Results represent the mean ± SEM and means of three and two separated experiments with duplicate determinations, respectively.

Figure 6. (A) and (B): Inhibitory kinetic analysis of the inhibition of CYP1B1-catalyzed 7-ethoxyresorufin *O*-deethylation activity by 10-hydroxyrutaecarpine. (A) the velocity (*v*) *versus* of rutaecarpine concentration (*S*) plots of CYP1A1-catalyzed rutaecarpine hydroxylation at the presence of 0 (○), 0.1 (●), and 0.2 (▲) μM 10-hydroxyrutaecarpine. Solid lines represent the lines as determined by non-linear regression analysis. (B) the Lineweaver-Burke plot. Solid lines represent the lines as determined by linear regression

analysis. (C): Binding spectra of 10-hydroxyrutaecarpine (1, 2, 3, 4, 5, and 7 μM) with CYP1B1 in 0.1 M potassium phosphate buffer, pH 7.4 at room temperature.

Figure 7. Rutaecarpine hydroxylations by human P450 forms.

Table 1. Effects of P450 inhibitors on rutaecarpine hydroxylation activity in human liver microsomes.

Inhibitor	The formation rate of rutaecarpine metabolites, % of control			
	10-hydroxyrutaecarpine	11-hydroxyrutaecarpine	12-hydroxyrutaecarpine	3-hydroxyrutaecarpine
α-Naphthoflavone	72 ± 3	46 ± 4	40 ± 14	49 ± 5
Orphenadrine	88 ± 2	90 ± 6	70 ± 9	83 ± 4
Sulfaphenazole	82 ± 3	88 ± 3	86 ± 6	75 ± 4
Quinidine	45 ± 15	47 ± 27	45 ± 28	42 ± 20
4-Methylpyrazole	84 ± 7	85 ± 8	79 ± 13	81 ± 9
Ketoconazole	14 ± 3	46 ± 19	55 ± 20	22 ± 8

Results represent mean ± SEM of three human liver samples. Rutaecarpine concentration was 200 μM in the assay. P450 inhibitors were added simultaneously with rutaecarpine in the assay as described in Methods.

Table 2. Rutaecarpine hydroxylation activities of human P450s expressed in *E. coli.*

	Rutaecarpine hydroxylation, pmol/min/nmol P450			
P450 form	10-Hydroxyrutaecarpine	11-Hydroxyrutaecarpine	12-Hydroxyrutaecarpine	3-Hydroxyrutaecarpine
1A1	1258 ± 125	1040 ± 37	885 ± 32	825 ± 9
1A2	n.d.*	181 ± 32	78 ± 11	31 ± 10
1B1	217 ± 22	n.d.	n.d.	29 ± 3
2A6	n.d.	n.d.	n.d.	n.d.
2C9	48 ± 10	139 ± 13	93 ± 19	98 ± 2
2D6	67 ± 22	173 ± 30	56 ± 4	86 ± 15
2E1	n.d.	112 ± 21	n.d.	n.d.
3A4	107 ± 41	n.d.	n.d.	117 ± 46

E. coli membranes expressing CYP1A1, CYP1A2, and CYP1B1 had 7-ethoxyresorufin *O*-deethylation activities of 41.7, 1.44, and 4.41 nmol/min/nmol P450, respectively. *E. coli* membranes expressing CYP2A6, CYP2C9, CYP2D6, CYP2E1, and CYP3A4 had oxidation activities toward their model substrates (as indicated in parenthesis) were 0.32 (coumarin), 11.6 (tolbutamide), 3.20 (dextromethorphan), 4.10 (chlorzoxazone), and 13.6 nmol/min/nmol P450 (nifedipine). Results represent mean ± SEM of three independent determinations with duplicated incubation. *n.d.: not detectable.

DMD Fast Forward. Published on February 24, 2006 as DOI: 10.1124/dmd.105.007849
This article has not been copyedited and formatted. The final version may differ from this version.

Figure 1

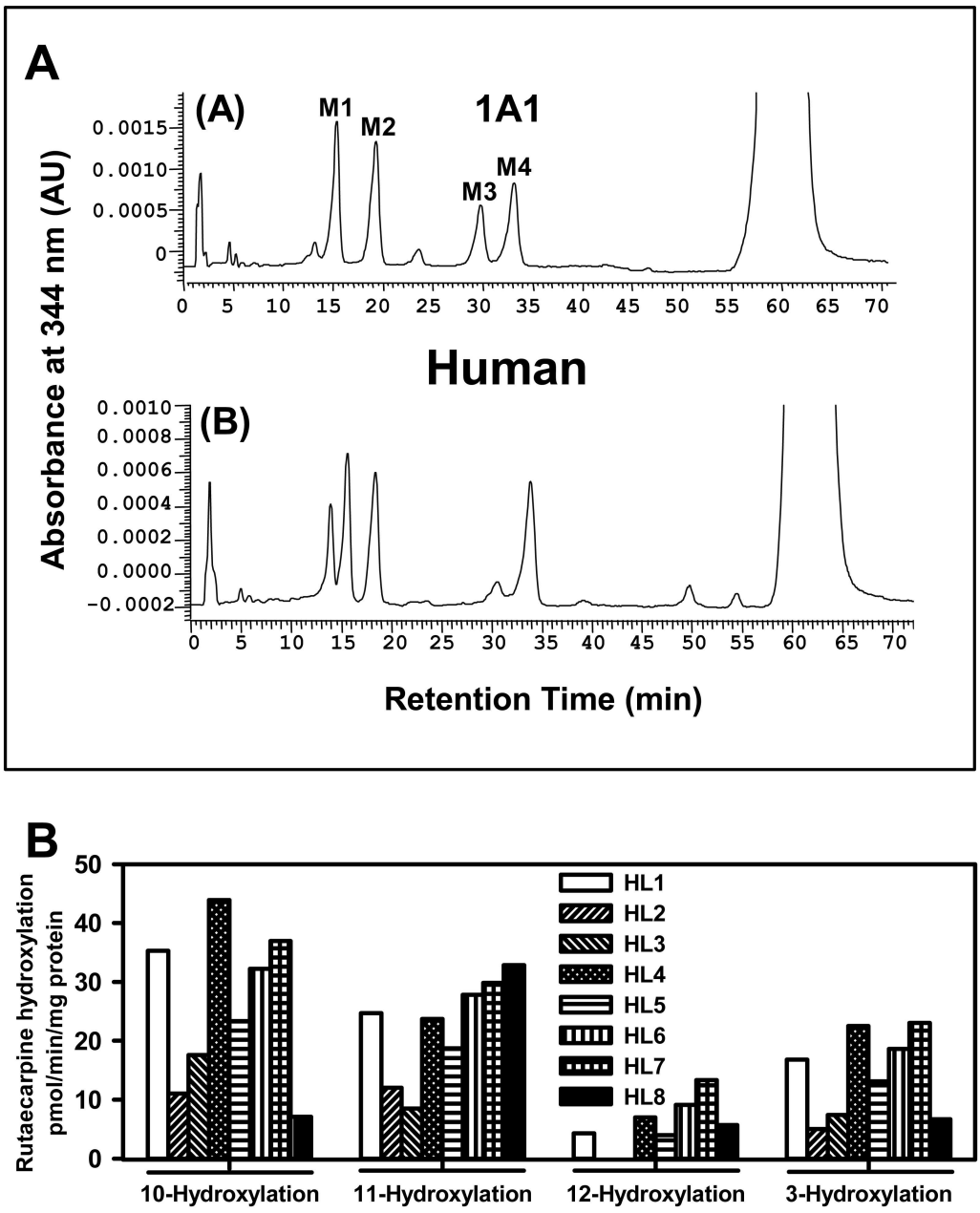

Figure 2

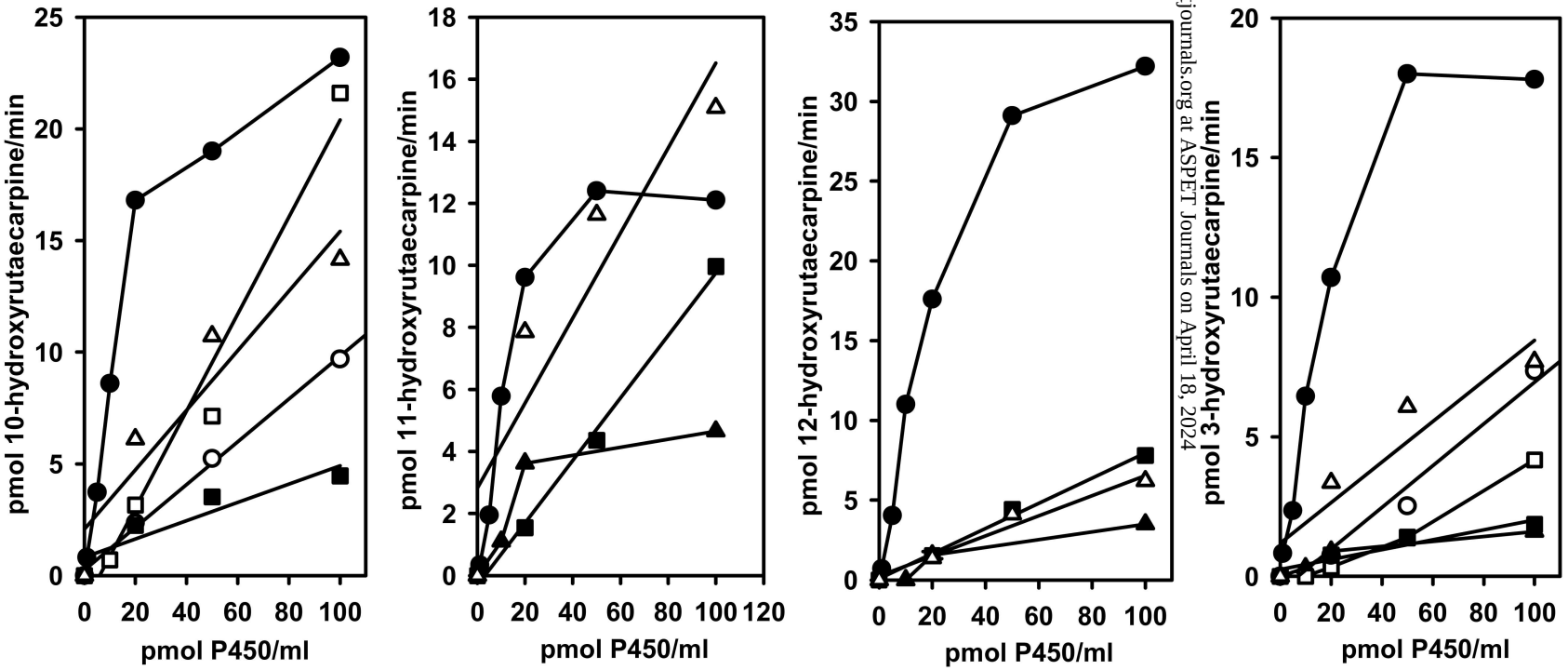

DMD Fast Forward. Published on February 24, 2006 as DOI: 10.1124/dmd.105.007849

Figure 3

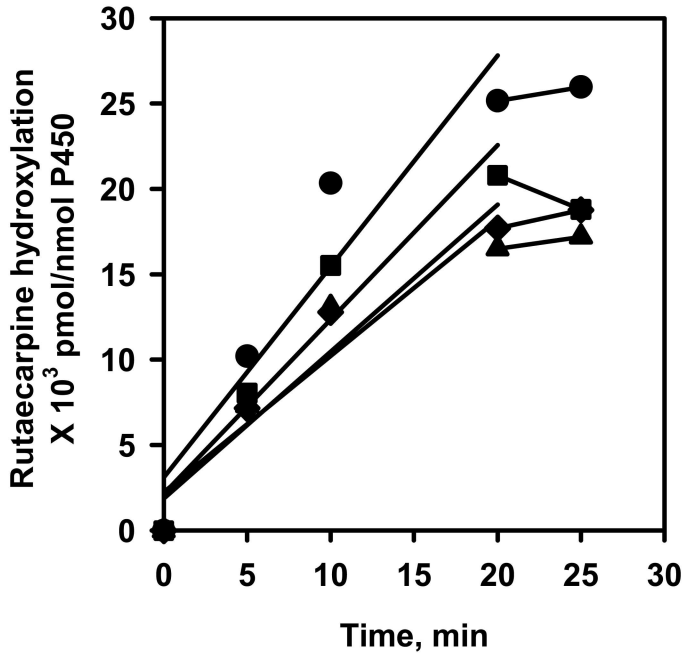

Figure 4

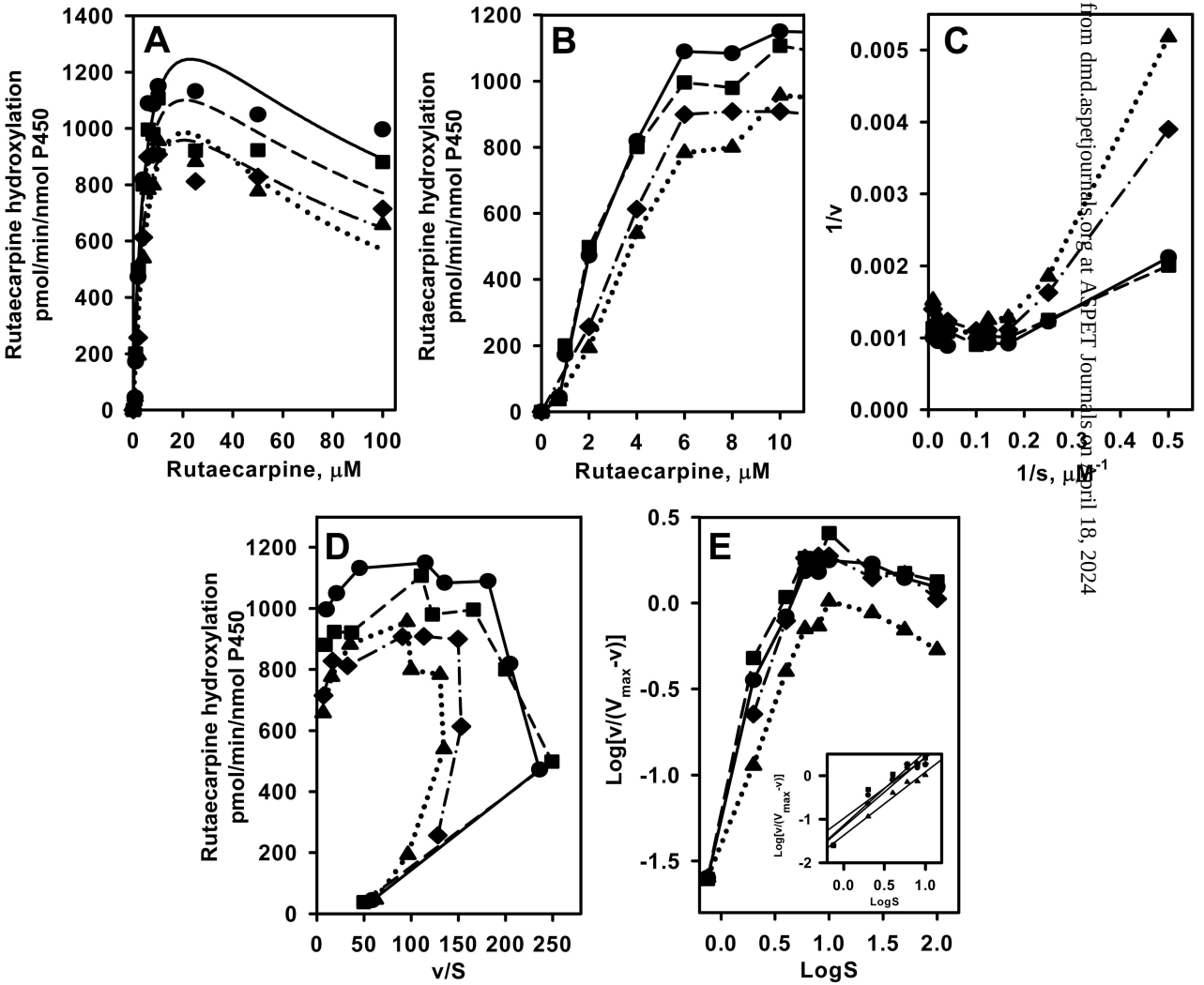

DMD Fast Forward. Published on February 24, 2006 as DOI: 10.1124/dmd.105.007849

Figure 5

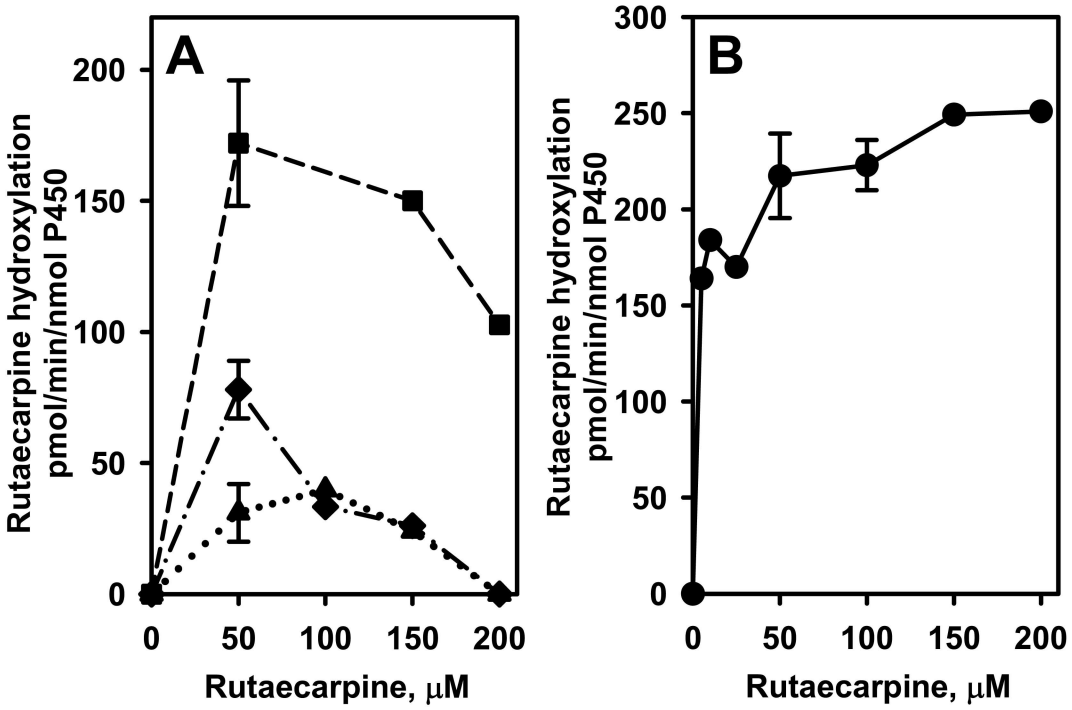

DMD Fast Forward. Published on February 24, 2006 as DOI: 10.1124/dmd.105.007849
This article has not been copyedited and formatted. The final version may differ from this version.

Figure 6

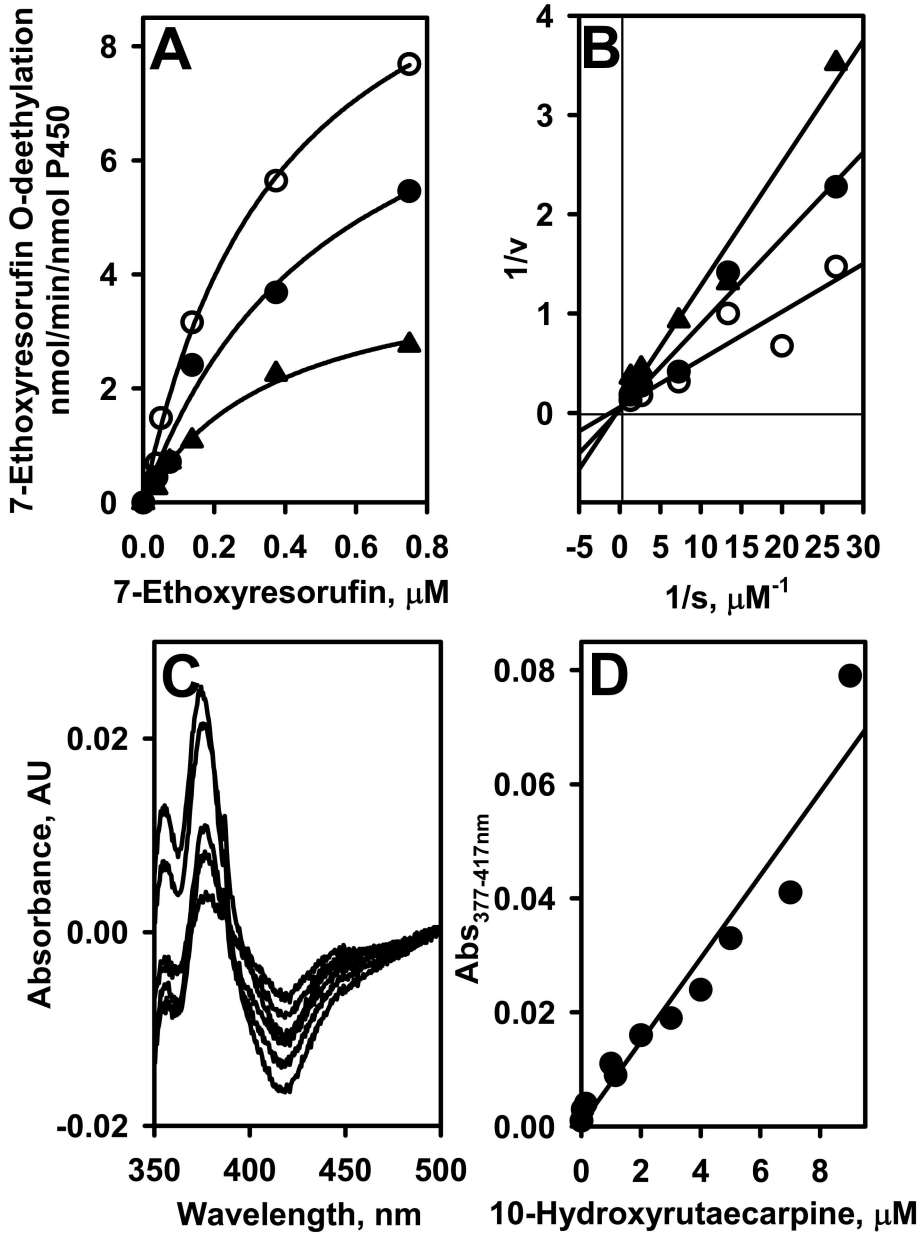

Figure 7